Validating Remote Sensing Data Along S-199 Cruise Track Using *In Situ* Chlorophyll, Carbon and Irradiance Measurements

Seth Bushinsky, Okorie Puryear, Simon Yang

Abstract

Remote sensing imagery is a potentially powerful tool for understanding global-scale ocean processes. Recent advances have enabled remote sensing imagery to estimate chlorophyll concentration in ocean waters and this has been used as a proxy for primary production. It is important to establish the exact relationships between satellite data and *in-situ* measurements to verify the accuracy of these assumptions.

This study tested the hypotheses that remote sensing derived chlorophyll values would be more accurate in eutrophic waters than oligotrophic waters and that the remote sensing imagery would fail to accurately estimate standing stock of carbon.

Our data show that remote sensing imagery can be used as an accurate proxy for *in-situ* chlorophyll measurements both at the surface and at depth. This is possible due to the high correlation between surface chlorophyll values and the depth of the chlorophyll maximum as well as the total integrated chlorophyll. Additionally, the satellite data is more accurate in oligotrophic waters than eutrophic waters.

However, analysis of *in-situ* particulate organic carbon values yielded chlorophyll to carbon ratios that varied by depth and by latitude. This fact casts doubt on the estimation of standing stock of carbon biomass and subsequently primary production by remote sensing.

Introduction

Primary production is the basic element incorporating inorganic carbon into the food chain. Accurate measurements of primary production are important for food-web dynamics and climate models. In the ocean, phytoplankton are the primary producers that feed species higher on the food chain. Without accurate measurements of phytoplankton on a large scale, it is very hard to determine the potential productivity of a system and the amount of other organisms that could be supported.

Primary production is also very important to understand, due to its impacts on the carbon cycle. Given the current uncertainties surrounding carbon export by primary producers, good measurements of primary production are important to many areas of research, especially climate change.

Remote sensing has become available over the last several decades. Satellites can currently obtain large-scale pictures of the ocean color (Figure 1). This ocean color data can be used to determine surface chlorophyll concentrations. Chlorophyll concentrations are used to estimate primary production according to assumed chlorophyll to carbon ratios. (Antoine et al. 1996, Iverson et al. 2000). One specific example of a model of primary production that is based on ocean color data is the Vertically Generalized Production Model (Behrenfeld and Falkowski 1997).

Remote sensing is still a new science and these models have several potential levels of inaccuracy. Working from the satellite down to the phytoplankton, the first potential inaccuracy is atmospheric distortion of ocean color radiation. MODIS data analysis is designed to take this into account; however, it is possible that not enough *in situ* measurements have been taken to fully correct for this distortion (Esaias et al. 1998).

One of the largest areas for potential error is inherent in the nature of remote sensing. Satellite data from color measurements is only derived from the first few meters of ocean (Babin et al. 1996). This does not cover the entire photic zone and potentially misses the chlorophyll maximum and large portions of primary productivity. Attempts have been made to refine ocean color estimates of primary production by incorporating physical parameters such as sea surface temperature into models (Bouman et al. 2003).

This uses factors that affect phytoplankton growth to improve the accuracy of primary production estimates.

A third level of error in using ocean color data as a proxy for primary production is that different phytoplankton communities will photoacclimate to their environmental light levels. Phytoplankton in areas of high light and will usually have fewer chlorophyll to prevent photoinhibition and those in low-light environments will have more to better utilize all available light. High light levels beneath the surface are often found in oligotrophic waters where water turbidity is low and low subsurface light levels are often found in nutrient-rich waters. This results in variable chlorophyll to carbon ratios dependent on the physiological properties of the phytoplankton (Arrigo et al. 2000). Currently, satellite-derived estimates of primary production poorly match *in situ* observations (Siegel et al. 2001, Campbell et al. 2002, Behrenfeld et al. 2005).

Some work has been done to validate remote sensing data using *in situ* measurements. However, this has been done on very localized scales. The objective of our project will be to use in situ measurements of chlorophyll, and carbon data to continue to validate remote sensing algorithms that use ocean color to estimate primary productivity. Our data collection will span a gradient of nutrient richness that will exhibit a wide range of chlorophyll and carbon concentrations. This will allow us to compare the accuracy of our *in situ* data to the data available from remote sensing. We hypothesize that the remote sensing data will not accurately predict *in situ* chlorophyll. Furthermore, the inaccuracy will likely be greatest in oligotrophic waters. These waters have the chlorophyll max furthest from the surface that is unlikely to be detected by satellite sensors. Also, we hypothesize that using ocean color data as a proxy for primary

productivity is inaccurate due to the variability that we expect to find in the chlorophyll to carbon ratio.

Methods

Hydrocasts and surface stations were preformed along the initial leg of our cruise track south from Honolulu. Particulate organic carbon (POC) and chlorophyll were obtained from both hydrocasts and surface stations. Satellite chlorophyll data was also collected for each station.

Surface Stations

Surface station samples were collected from flow-through sea water at 0000, 0400, 0800, 1600 and 2000. Two 500 ml samples (a and b) were collected for chlorophyll samples at each station. Also, one 2 L water sample was collected for POC with replicates taken at 0400 and 1600.

Hydrocasts

Eight hydrocasts were deployed at noon along the cruise track (table 2). Each hydrocast consisted of a Conductivity Temperature and Depth sensor (CTD), fluorometer and 13 Niskin bottles for collecting water samples. Twelve of the bottles were tripped in pairs, yielding one 2L POC sample and two 500 ml chlorophyll samples per depth. Additionally, a surface sample was taken using the same technique as the surface stations.

Firing depths were pre-set with the intention of bracketing the chlorophyll maximum. For each hydrocast a secchi disk was deployed beforehand in an attempt to establish the 18% light level. These data were largely ignored in favor of previous fluorometer profiles to determine bottle trigger depths.

Chlorophyll Filtration and Analysis

Each chlorophyll sample was filtered through Whatman 0.45 um glass filters, placed in cuvettes and frozen. All chlorophyll samples were processed en masse at the Palmyra Research Station on Palmyra Atoll. 7 ml of acetone were added to dissolve the chlorophyll and the filter. Samples were centrifuged and then read twice by a calibrated fluorometer. Each pair of readings was averaged to determine the chlorophyll concentration for the sample. This method is an SEA modification of the fluorometric determination of Chlorophyll from Parsons et al.

Hydrocast replications were used to determine the percent error between two samples from the same parcel of water as a proxy for the error present in our sampling techniques. The average error for hydrocast chlorophyll replicates was 25%. Percent error for surface station replicates was also calculated to get a picture of the patchiness present in our sampling locations. Percent error for surface station chlorophyll chlorophyll replicates was 35%.

Integrated chlorophyll values were obtained using a trapezoid integration method.

Particulate Organic Carbon Filtration and Analysis

Water samples taken for particulate organic carbon (POC) analysis were filtered through pre-combusted glass fiber filters. Each filter was then dried in a Petri dish. Once dry, the filter was then folded and packed in pressed-tin boats. The packed tin boats were flown from Palmyra to Stanford University for gas chromatography analysis. POC values and particulate organic nitrogen (PON) values were obtained for each sample.

Satellite Chlorophyll Values

MODIS ocean color-derived chlorophyll data was downloaded for the time period and geographic location of our sampling stations. Each satellite picture was an eight-day composite. For each station, the composite with the closest end day was used to determine chlorophyll concentrations. Satellite-derived chlorophyll concentrations were obtained for the specific latitude and longitude coordinates of each station using a two-dimensional interpolation function that weights the values of the nearest data points in the satellite image.

Results

Appendix A lists the date, time, ship's taffrail log and GPS location of where each chl-a and POC surface station was sampled. Since replicate POC samples were made each day at 0400 and 1600, an "a" or "b" is used to distinguish the two in the Station # column.

Appendix B lists the date, time, ship's taffrail log and GPS location of where each hydrocast was completed.

Appendix C contains hydrocast data consisting of depth, two replicate chlorophyll values (A and B), their average Chl-a value, percentage of difference between the replicates, PON, POC , C:N ratios and corresponding satellite chl-a values for each bottle of all the Hydrocasts.

Appendix D contains surface station data consisting of two replicate chlorophyll values, their average Chl-a value, % difference between the replicate Chl-a, POC, Avg POC, % difference between replicate POC, PON, avg PON, C:N ratios and corresponding satellite chl-a values for each surface station. Surface station numbers with "a" and "b" have replicate POC/PON values for the same station number.

Appendix E contains the integrated chlorophyll concentration, integrated chlorophyll concentration calibrated with the fluorometer and the surface chlorophyll concentration for each hydrocast. It also contains the correlation coefficient between satellite chlorophyll values and the hydrocast surface station (bottle 13), satellite chlorophyll values and integrated chlorophyll concentration, as well as satellite chlorophyll values and integrated chlorophyll concentration calibrated with the fluorometer.

Surface Stations

Figure 1 plots chlorophyll-a values from *in-situ* measurements and those obtained from satellite imagery against latitude. This shows the similar shape of the two plotted series.

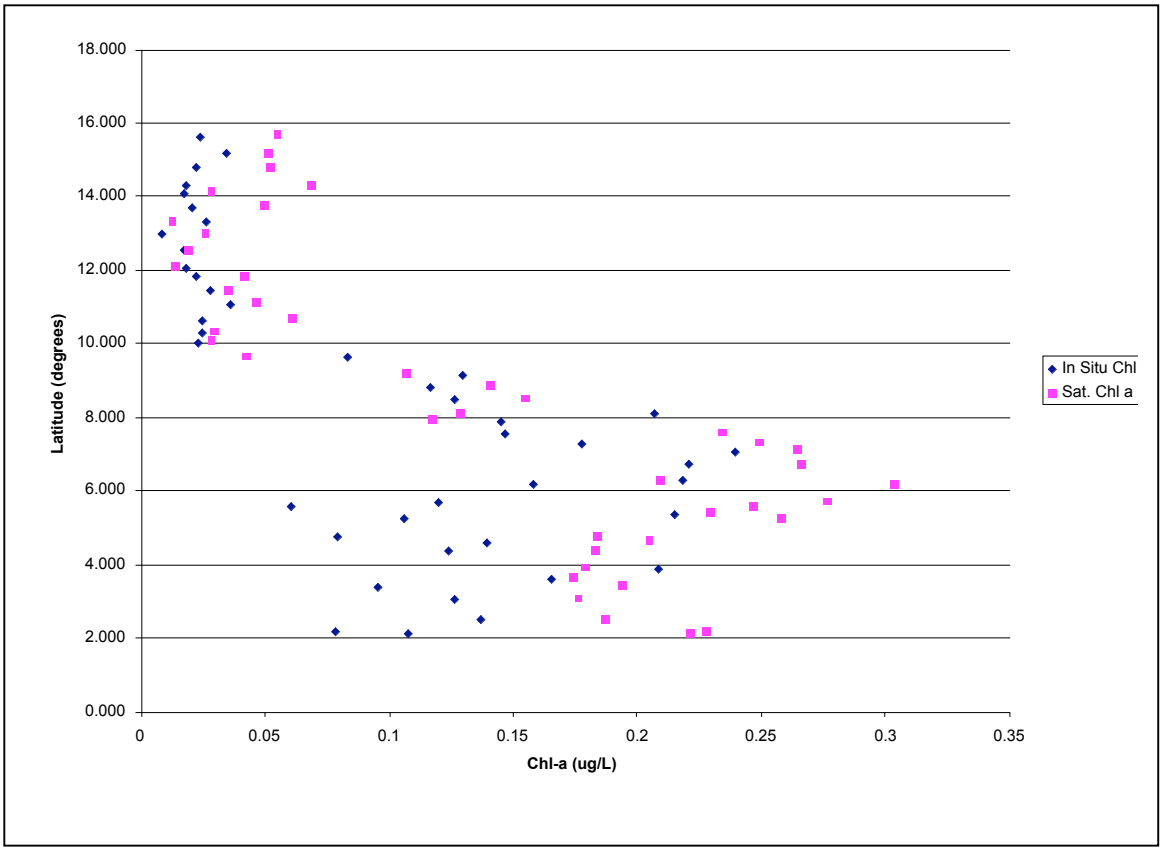

Fig 1. Latitude vs In situ surface station Chl-a and satellite Chl-a

In-situ Chl-a surface station samples were plotted against respective satellite values (Figure 2). Chl-a estimates from *in-situ* measurements and remote sensing had a correlation of 0.82. The correlation was better in latitudes north of 10 10°N and worse between 10 degrees and 3 degrees. A linear trendline fit with an R^2 of 0.67. Expected satellite values were then predicted using this equation. The difference between actual and predicted satellite chlorophyll values was then plotted against latitude (Figure 3).

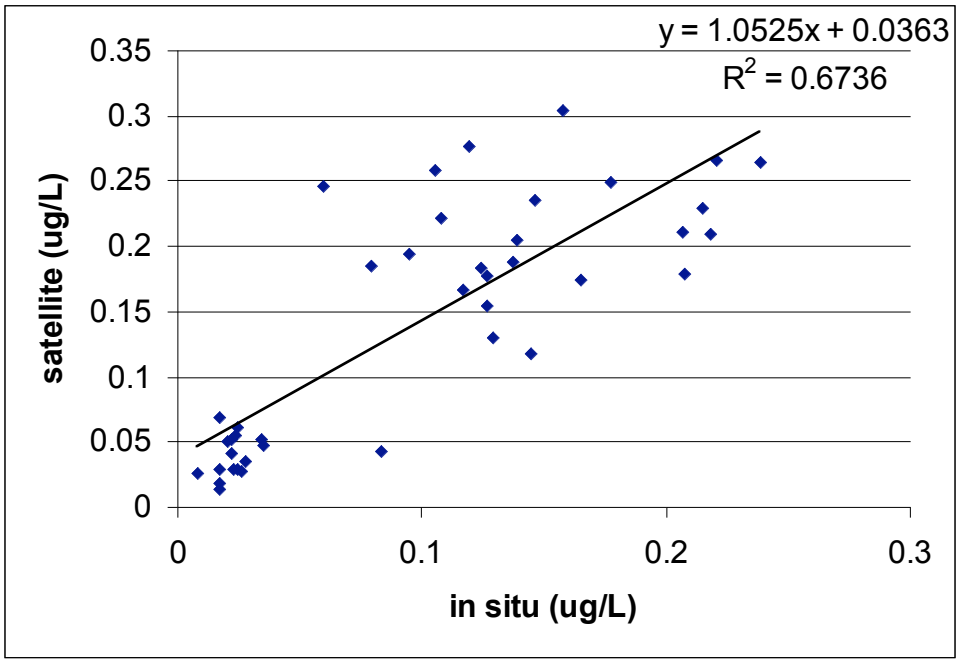

Fig 2. *In-Situ* surface station vs. satellite.

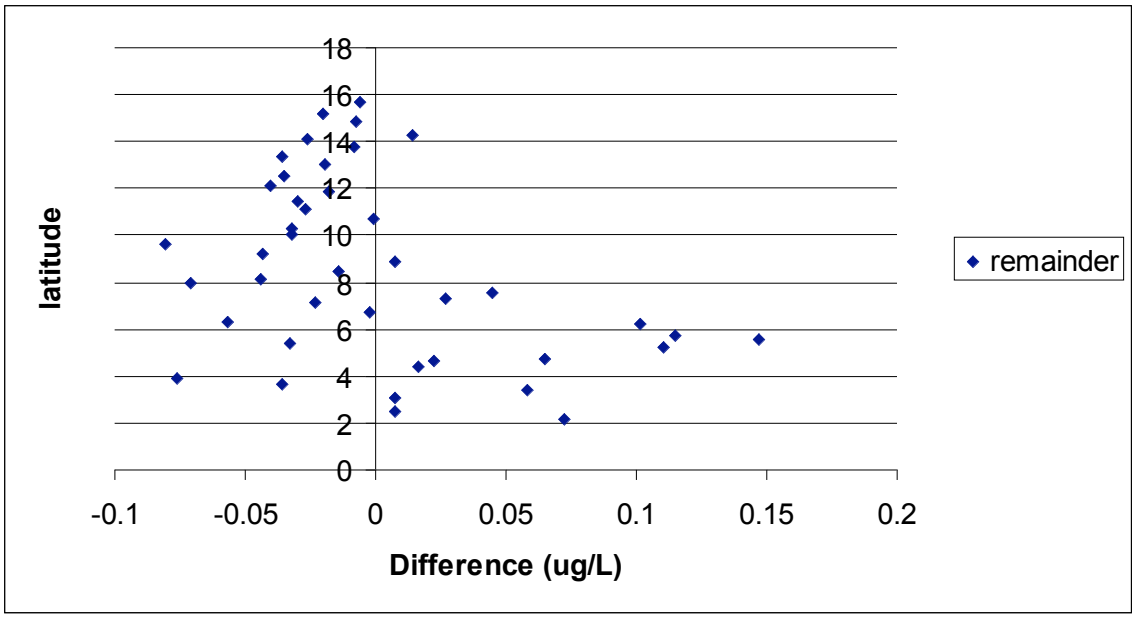

Fig 3. Satellite Chl-a values minus predicted Satellite values.

Depth of the chlorophyll max compared to *in-situ* surface chlorophyll values from each hydrocast show an inverse linear relationship (Figure 4). Depth of Chlorophyll max for each hydrocast (as derived from the CTD fluorometer) and satellite chlorophyll values were plotted against latitude (Figure 5). Satellite chlorophyll values followed the same trend as chlorophyll max depth values. Satellite Chlorophyll values were then plotted against chlorophyll max depth for all hydrocasts except HC-32 which did not have a corresponding satellite value(Figure 6). A linear fit was made with an R^2 value of .93.

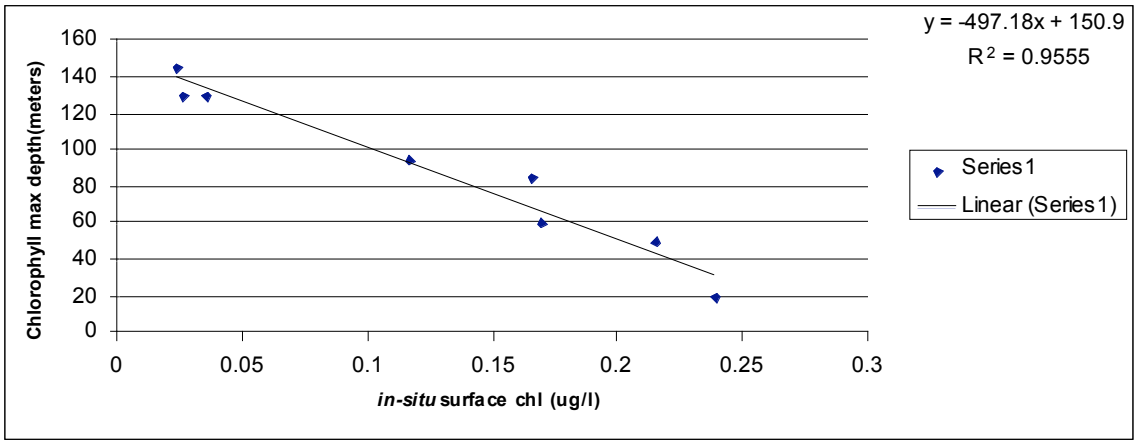

Fig 4. Chlorophyll max depth(meters) vs *in-situ* surface chlorophyll measurements from Hydrocast data

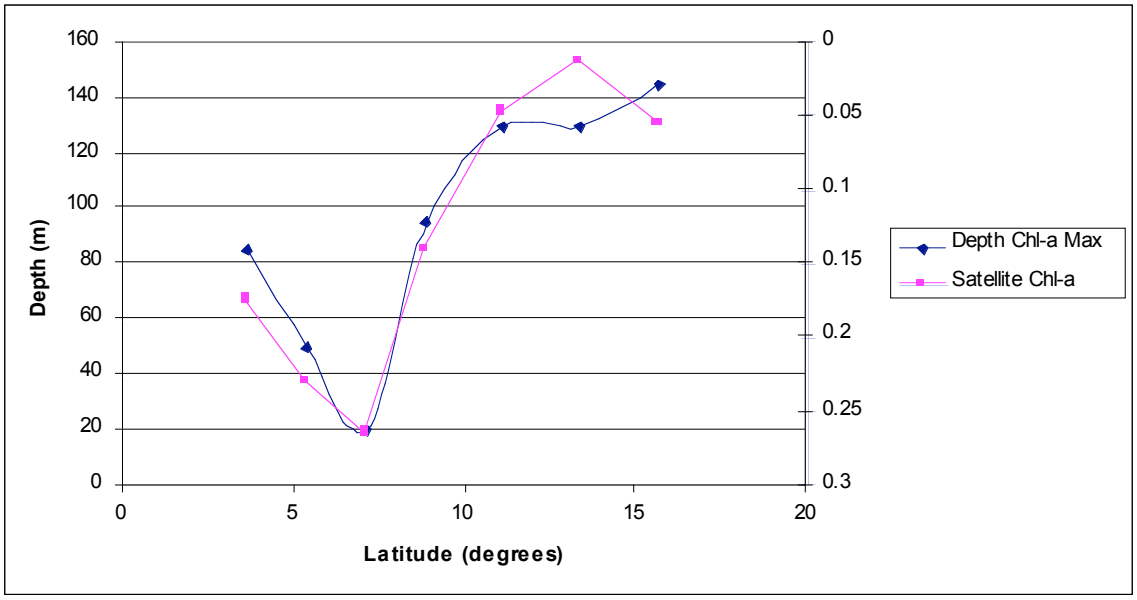

Fig 5. Depth Chl-a Max and Satellite values vs Latitude

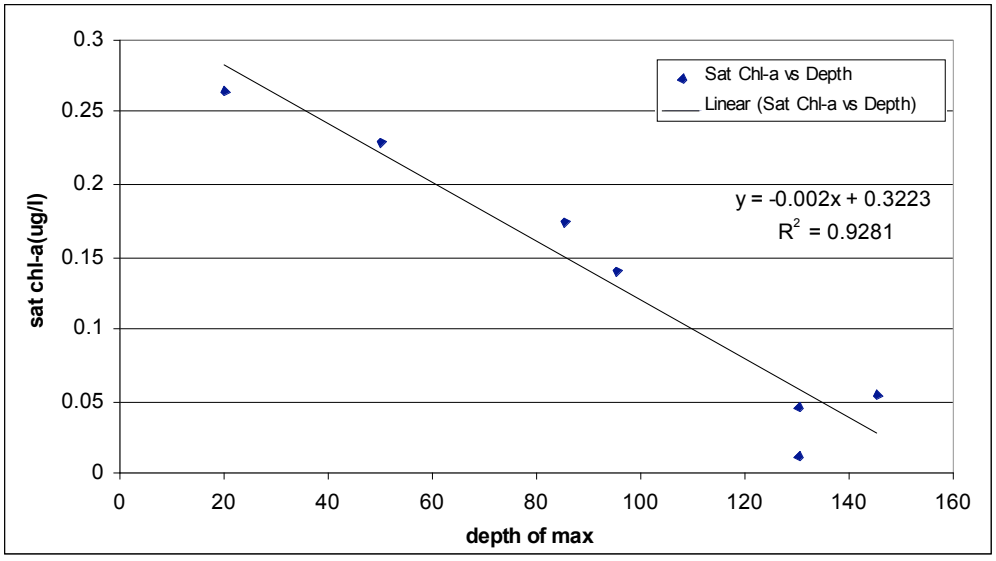

Fig 6. Depth Chl-a max vs Satellite values

A comparison was

made of fluorometer values to actual chlorophyll values for all hydrocast bottles excluding bottle 13, which were done as surface stations (Figure 7). A correlation of 0.915 was found. The best fit trendline with R^2=0.838 was found. Based on the high correlation and R^2 value, we were able to calibrate our in-vivo fluorometer to its corresponding Chl-a values and produce a more complete Chl-a depth profile using the above relationship. Both the sampled Chl-a depth profile and calibrated Chl-a depth

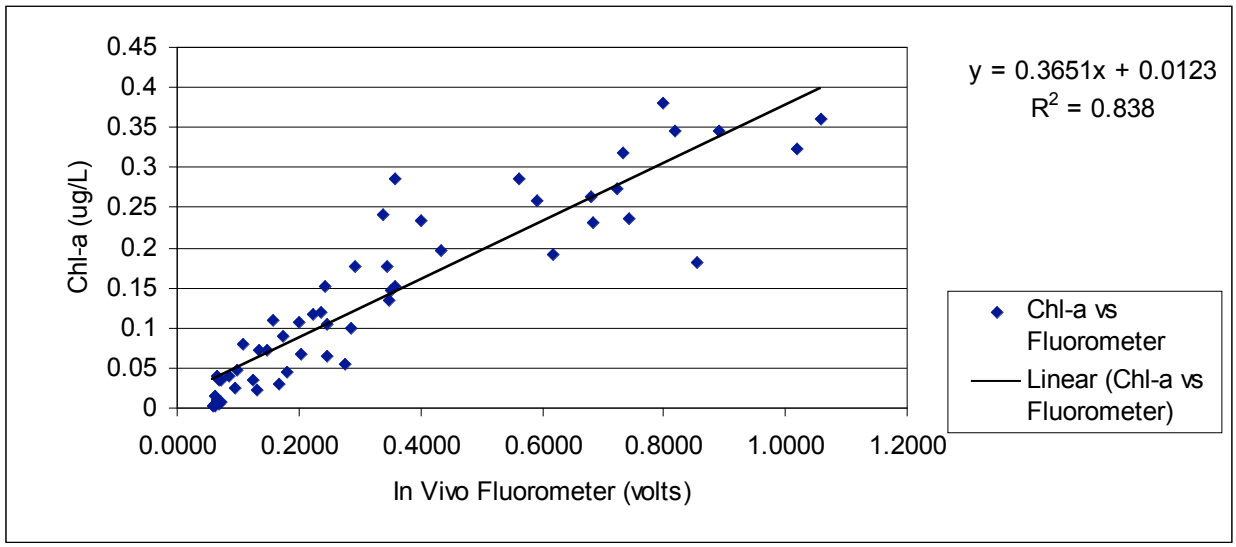

Fig 7. In Vivo Fluorometer (volts) vs Chl-a (µg/l) for Hydrocast no

profile were integrated using trapezoid rule down to 500m and displayed in table 5. Satellite surface values, depth integrated chlorophyll, and depth integrated chlorophyll from fluorometry values were plotted against latitude (Figure 8). Calibrated values varied in a similar pattern as that of the chlorophyll based integrations. Integrated Chlorophyll values were higher in both calibrated and chlorophyll based data sets at latitiudes higher than 10ºN. They subsequently fall to lower levels approaching the Equator.

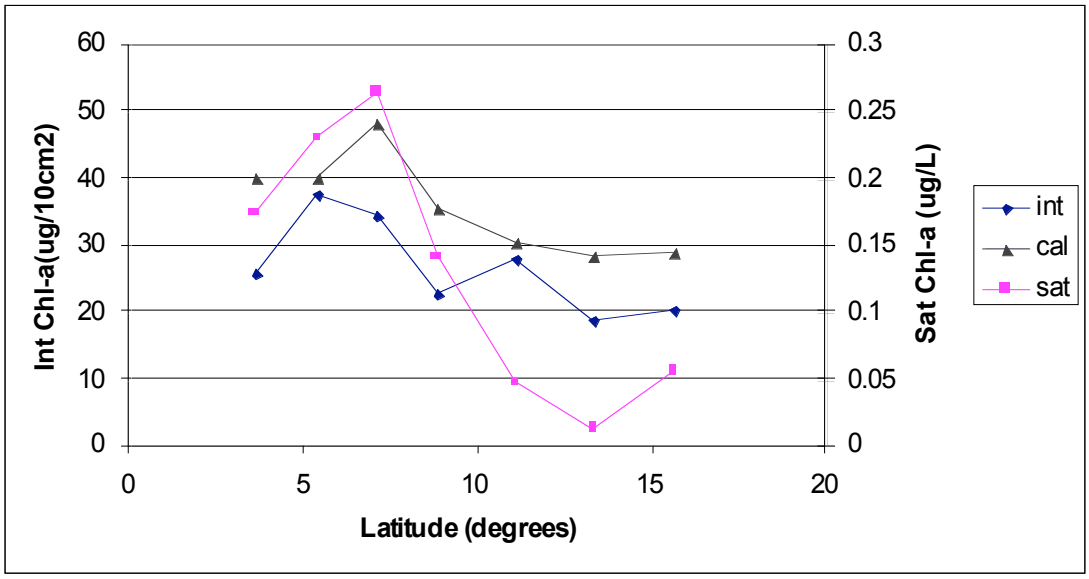

Fig 8. Integrated Chl, Calibrated Chl and Satellite values vs

Due to the higher resolution of the calibrated Chl-a profile and correlation to satellite values, a linear trendline was develop between the calibrated depth integrated Chl-a and satellite values with R^2=0.92. (Figure 9).

We also noticed high correlation of bottle 13 (surface sample) chl-a values to the satellite chl-a values,

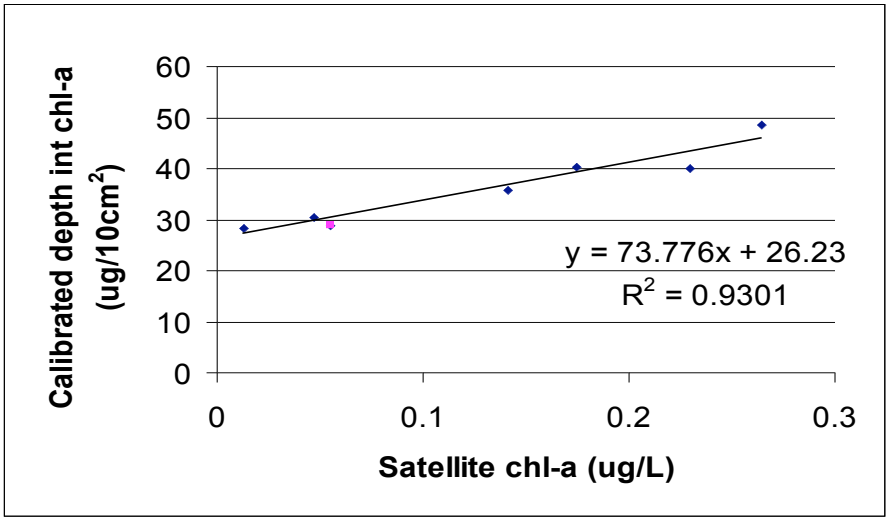

Fig 9. Calibrated depth integrated Chl-a vs Satellite chl-a

a linear fit was made between the two with R^2 =0.97. (Figure 10).

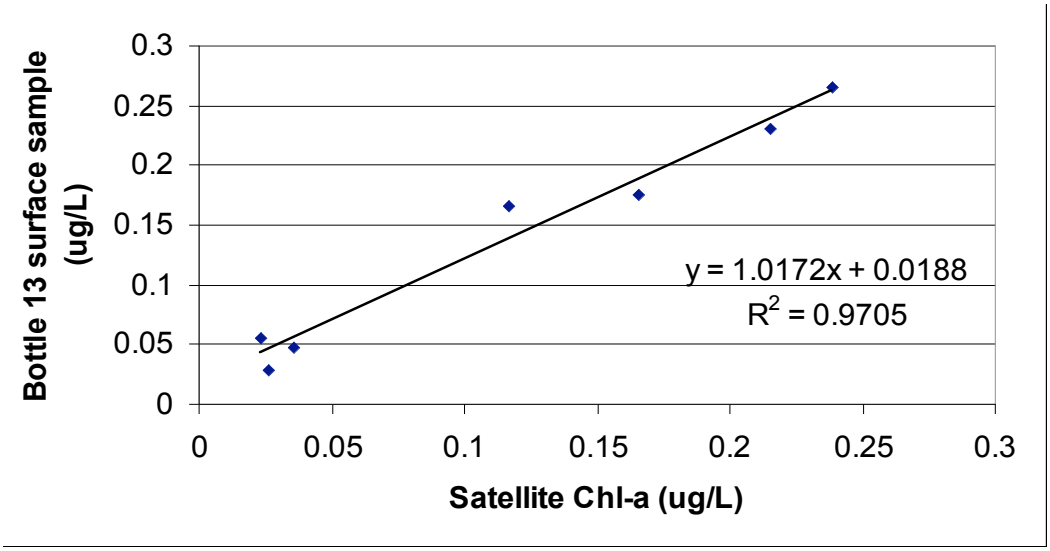

Fig 10. Comparison of satellite vs in-situ Chl-a

Particulate organic carbon

Hydrocasts 010, 013 and 016 (HC-010, HC-013, HC-016) occur in the latitudinal range of 15 degrees, 38.8 minutes north to 11 degrees, 5.6 minutes north (Figure 11). HC 010, 013 and 016 show a uniform density profile in the mixed layer depth, below which the pycnocline starts and the densities increase.

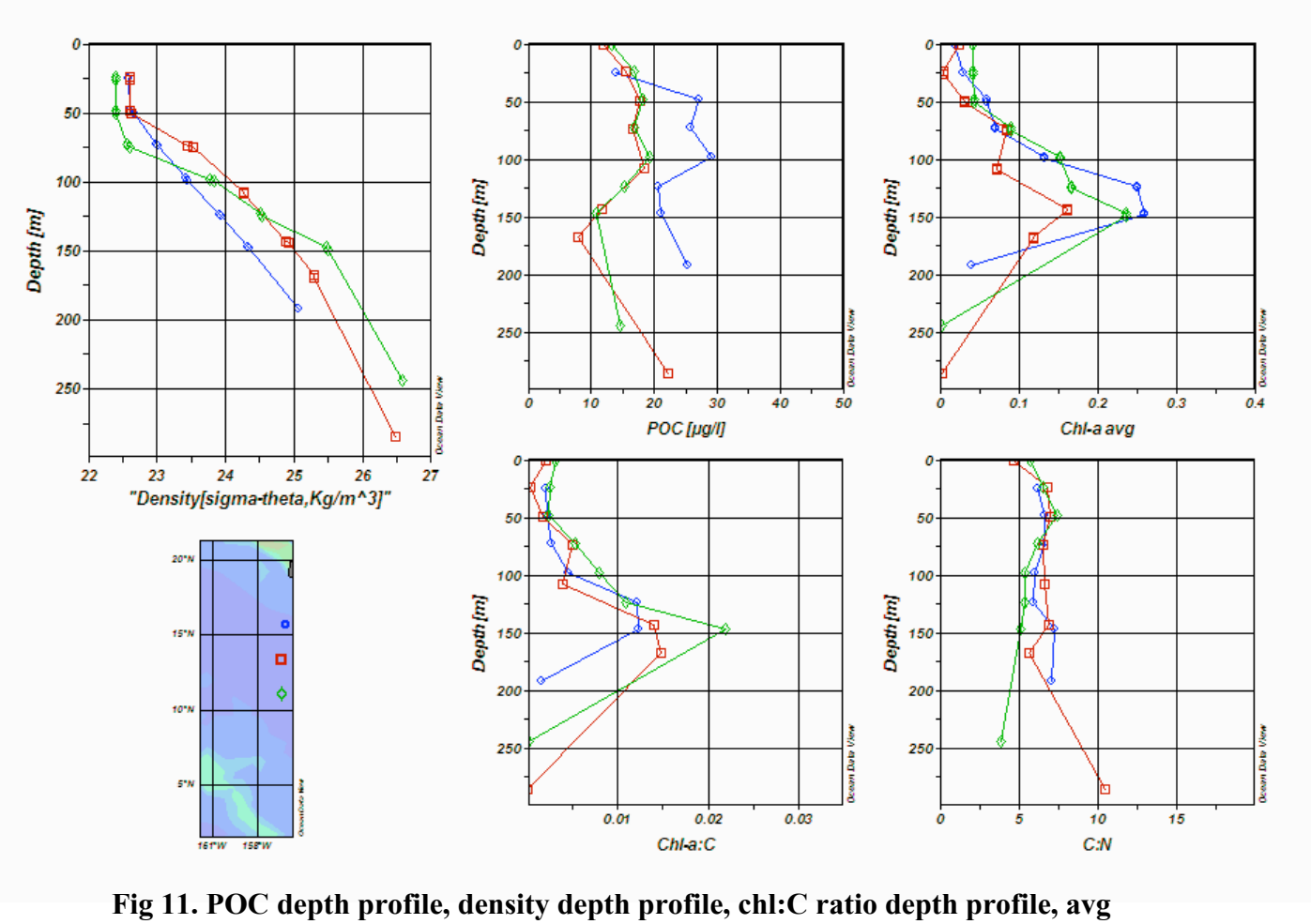

Fig 11. POC depth profile, density depth profile, chl:C ratio depth profile, avg chlorophyll depth profile, and C:N ratio depth profile for HC-010 (blue), HC-013 (red), HC-016(green)

HC-010, 013 and 016 all show dual particulate organic carbon (POC) peaks at around 50 and 100 m depth. The POC peaks for HC-013 and 016 are at approximately 18 µg/l and the POC peaks for HC 010 are 27 µg/l at 50 m and 29 µg/l at 100m. The depth of chlorophyll maximum is between 140 and 150 m for all three hydrocasts. The chlorophyll maxima range from 0.15 to 0.25 µg/l.

All three hydrocasts show increasing chlorophyll to carbon ratios (Chl-a:C) beneath the first 25 m until the peak, after which the ratio decreases. HC-010 has a peak in Chl-a:C of .012 between 125 and 150 m. The Chl-a:C ratio of HC-013 has a peak of .022 at 170 m and HC-016 a peak of .015 at 150 m. Carbon to Nitrogen ratios (C:N) are between 5 and 7, except for the deepest bottles of HC-013 and HC-016 which are at 10.3 and 3.7, respectively.

Hydrocasts 020 and 023 (HC-020, HC-023) were deployed at 8 degrees, 50.5 minutes north and 7 degrees, 6.2 minutes north (Figure 12). HC-020 and 023 show a uniform density profile until 75 m, below which the pycnocline starts and the densities increase.

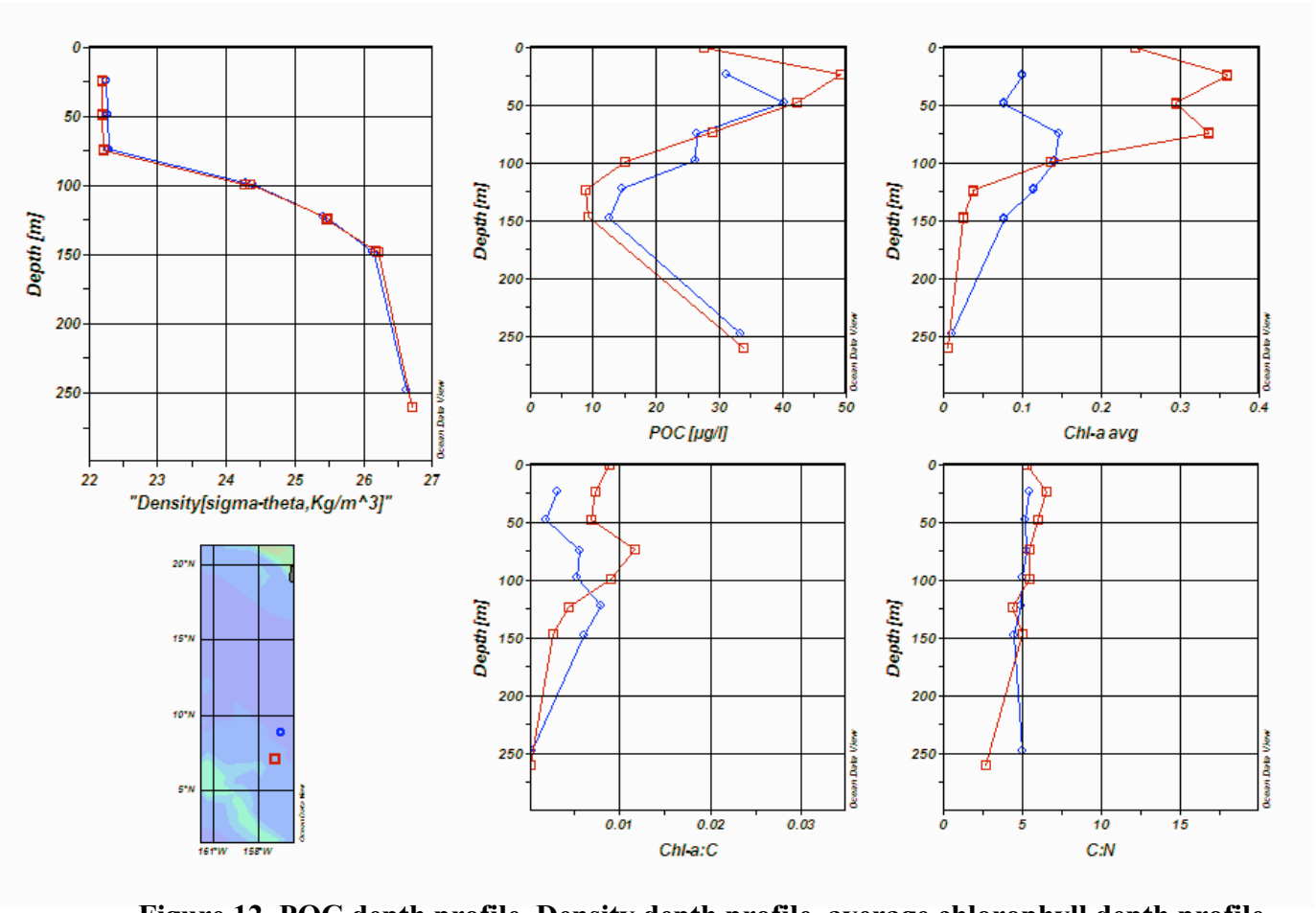

Figure 12. POC depth profile, Density depth profile, average chlorophyll depth profile, chl:C depth profile, and C:N depth profile for HC-20(blue) and HC-23(red)

HC-020 and 023 show peaks in POC at around 50 and 25 m depth. The POC peaks for HC-020 and 023 are at 40 and 50 µg/l, respectively. The depth of chlorophyll maximum of HC-020 is between 75 and 100 m. The depth of chlorophyll maximum of HC-023 is between 25 and 75 m. The chlorophyll maxima of HC 020 and 023 are at 0.14 and 0.35 µg/l, respectively.

The Chl-a:C ratios decrease at first, then increase to a peak before decreasing again in deeper waters. HC-020 has a peak of 0.008 at 125 m. HC 023 has a Chl-a:C peak of 0.012 at 75 m. C:N ratios are centered around 5. The C:N ratio of the 260 m

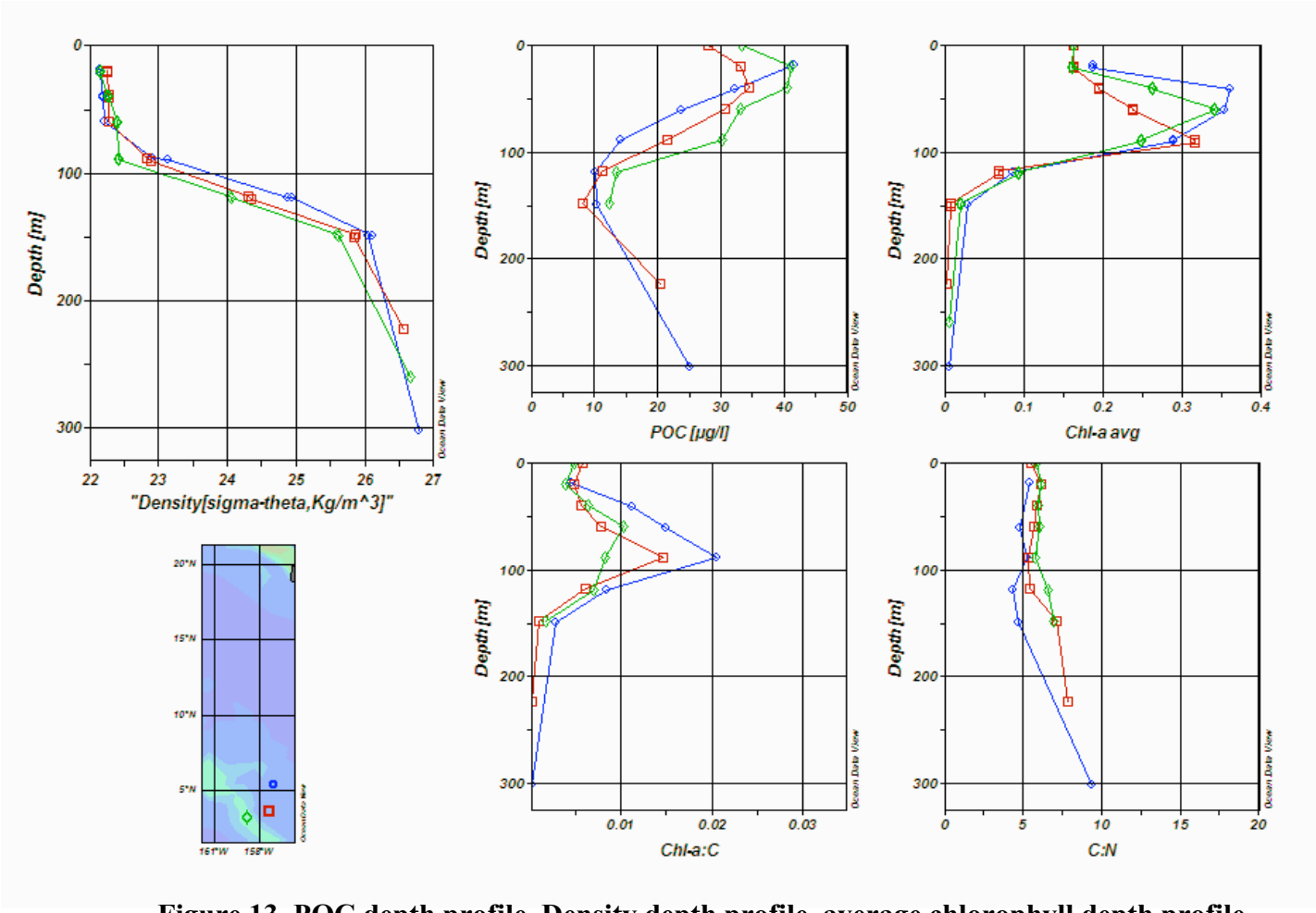

Figure 13. POC depth profile, Density depth profile, average chlorophyll depth profile, chl:C depth profile, and C:N depth profile for HC-26, HC-29, and HC-32

bottle of HC 023 decreases to 2.7.

Hydrocasts 026, 029, 032 (HC-026, HC-029, HC-032) occur between 5 degrees, 23.5 minutes north and 3 degrees, 15.2 minutes north (Figure 13). HC-026, 029 and 032 show a pycnocline starting between 60 and 90 m. HC-026, 029 and 032 all show POC peaks between 19 and 39 m. The POC peaks for HC-026 and 032 are at approximately 41 µg/l and the POC peak for HC 029 is 34 µg/l.

The depths of chlorophyll maxima are 40 m for HC-026, 90 m for HC-029 and 60 m for HC-032. The chlorophyll maxima range from 0.32 to 0.36 µg/l. Beneath the first 25 m, all three hydrocasts show increasing Chl-a:C ratios until the peak, after which the ratio decreases. HC-026 has a peak in Chl-a:C of 0.021 at 90 m. HC-029 has a peak of 0.015 at 90 m. HC-032 has a Chl-a:C ratio peak value of 0.01 AT 59 m.

C:N ratios for the hydrocasts are between 5 and 7.8, except for the deepest bottle of HC 026 which is 9.4.

Chl-a:C ratios for surface stations between 15 and 10 degrees north ranged from 0.0003 and 0.002 (Figure). Chl-a:C ratios for surface stations between 10 and 3 degrees north ranged from 0.0015 and 0.009.

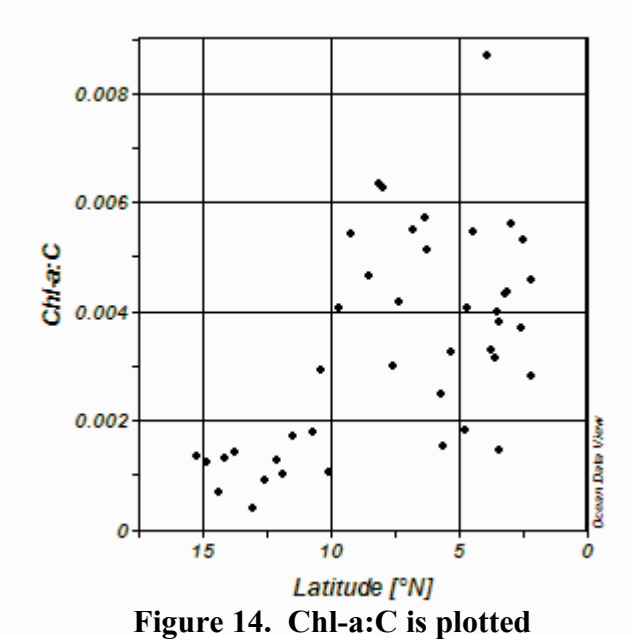

Figure 14. Chl-a:C is plotted against latitude for all of the surface sampling stations.

The average percent difference between duplicated POC measurements was 18.46%.

Discussion

Our results show some interesting trends and point rather clearly to the usefulness of satellite imagery in discerning phytoplankton productivity dynamics of the eastern Pacific Ocean. The close correlation between surface satellite values and in-situ chlorophyll surface values shows that the MODIS satellite accurately predicts surface chlorophyll concentrations. Nonetheless there are some interesting trends that arise from the data.

Accuracy of satellite imagery in oligotrophic vs eutrophic waters

Comparing the surface stations to satellite values (fig 1) is a far better measure of the accuracy of the satellite values than the comparison between the hydrocast surface stations and satellite values (fig 4). This is mainly due to the fact that the satellite can only see the topmost layer of the ocean.

Our first hypothesis was that there would be a discrepancy in the accuracy of the satellite depending on the productivity state of the water. We theorized that due to photoacclimation of the phytoplankton community in oligotrophic waters, the satellite would miss much of the chlorophyll present in the water column due to the increased depth of the chlorophyll max. This would be in contrast to more eutrophic waters where the chlorophyll max would be closer to the surface and therefore more likely to be incorporated into the satellite's picture of productivity. Ultimately our data proved otherwise. It is clear that there is a marked difference in the accuracy of the satellite above and below 10° N latitude (fig 1). In contrast to our hypothesis this difference in

accuracy favors the oligotrophic waters. The reason for this discrepancy is likely due to the patchiness of the eutrophic waters as opposed to the oligotrophic waters. When we sampled waters below 10° N we were leaving the center of the gyre and entering the fringes of equatorial upwelling zones where nutrients were being brought to the surface and increasing surface primary production. This phenomenon creates patchy areas of production that we passed through and sampled on our voyage south. The satellite in contrast samples a larger area and averages the data it receives to create value for that given pixel. Additionally, the satellite uses running eight day averages to create its pictures, which means it takes into account more of the change in the community than our one time sample of the location. This most likely led to the random variation between in-situ and satellite derived chlorophyll values at more southerly latitudes. Oligotrophic waters are more uniformly low in productivity with less surface patchiness. This is why our data above 10°N is more in line with what the satellite is seeing. The satellite-averaged value is comprised of consistent pictures of a relatively dead surface which matches with our surface samples.

Depth of the Chlorophyll max vs satellite surface chlorophyll value

It is of interest that the correlation between the depth of the chlorophyll max and satellite/*in-situ* derived surface chlorophyll values is almost 1:1. This means that if enough accurate measures of surface chlorophyll and the chlorophyll max depth are gathered then an equation that uses satellite, or *in-situ,* surface chlorophyll to predict chlorophyll max depth could be created. This would be very useful in future

oceanographic research, eliminating guesswork involved in determining depths at which to sample the chl max. By using the surface fluorometer to estimate surface chlorophyll values then plugging them into the equation we would be able to predict the chlorophyll max depth and thus inform our depth choices for the carousel bottles.

Another interesting trend is the progressive shoaling of the chlorophyll max depths as we moved southward along our cruise track. HC-010 and HC-016 have chlorophyll max depths of 145m and 130m this is in contrast to the much shallower depths of the chlorophyll max in HC-23 and HC-26. This trend is likely due to the change in the depth of the nutricline as we move further south towards the equatorial upwelling zone. As the nutricline shoals the majority of the phytoplankton community can remain closer to the surface while maintaining a high surrounding nutrient concentration to maintain compensation photosynthetic rates.

Chlorophyll values vs fluorometer measurements

The relatively good correlation between fluorometry values from the CTD and real chlorophyll values from all of our samples gives good confidence to our use of Fluorometry curves in the integration of total water column chlorophyll concentration at each of our hydrocast stations. This correlation is also valuable because it means that with the trendline calculated for the data in Figure 7 we could also use the carousel fluorometer aboard our vessel to extrapolate real chlorophyll values without the need for time consuming filtering and chemical reactions. The numbers would be prone to some

error but that error would not likely eclipse the average 35% error we had between our surface station replicates.

Integrated Chlorophyll vs Satellite measurements

Since we were limited to 7 bottles to sample the chlorophyll profile for each hydrocast, we used our calibrated in-vivo fluorometer measurements to integrate the chlorophyll depth profile. Figure 7 and Table 5 shows that the calibrated integrated chlorophyll correlate better to the satellite surface values then our measured chlorophyll profile alone. This is likely due to the uneven curve produced from our seven bottles. The calibrated fluorometer values for integrated chlorophyll are a better fit because they smooth the curve and account for any missing data points. Fig. 8 also shows that there is a linear relationship between what the MODIS satellite sees and the *in-situ* integrated chlorophyll.

Particulate Organic Carbon and Chlorophyll to Carbon Ratios

Hydrocasts 010, 013 and 016 were deployed in the more oligotrophic, northern waters of our cruise track. Each show dual POC maxima at around 50 and 100 m. The shallow POC maxima seem to correlate to the start of the pycnocline. A more accurate estimation of the pycnocline can be obtained by looking at the actual density data recorded by the CTD at 4 Hz than the discrete bottle samples. This shows that the pycnoclines of HC 010 and 016 do occur at approximately 50 m, but that the actual pycnocline of HC 013 is closer to 75 m (Figure 11). However, given that POC data is

only available where water samples were collected, it is possible that the first POC maximum of HC 013 is slightly below the recorded max. The correlation between the first POC maximum and the pycnocline seems to be present for these hydrocasts. This would result from an accumulation at the density change of organic matter settling out of the mixed layer.

The deeper POC maximum occurs at 100m for these three hydrocasts. This is 50 m above the chlorophyll maxima at 150 m. This shows that the chlorophyll maximum does not correspond to the depth at which the most primary production is occurring. Instead it appears that the most productive phytoplankton are at 100 m, while those at 150 m are at the threshold where photosynthesis production outweighs respiration. The high chlorophyll levels are indicative of photoacclimation by the phytoplankton; the amount of chlorophyll has been increased in response to low light levels and do not represent high production. The Chl-a:C ratios are highest at 150 m. This further provides evidence that phytoplankton at 150 m need very high levels of chlorophyll to survive, while those at 100 m have the highest levels of carbon without needing high amounts of chlorophyll.

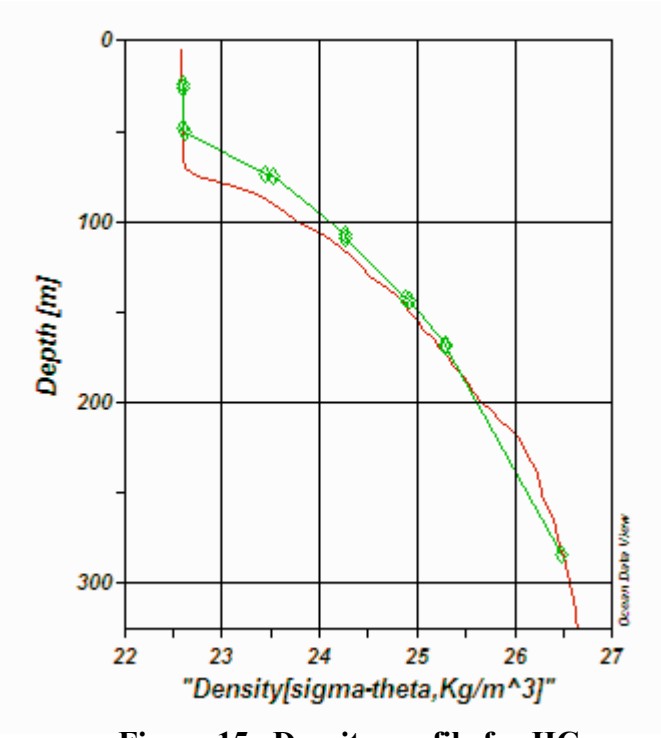

Figure 15. Density profile for HC 013 derived from discrete bottle data compared to the CTD profile.

Hydrocasts 026, 029 and 032 were deployed near the Line Islands in more eutrophic waters. Their carbon profiles are significantly different than those of the oligotrophic hydrocasts. The POC profile shows only one maximum per cast. This peak occurs well above the pycnocline in all instances. This indicates that the phytoplankton in these areas are not as nutrient limited as those in the first three hydrocasts and do not need to live near the pycnocline to acquire the necessary nutrients. Also, both the POC peak and the chlorophyll peak are present at much shallower depths than those in the oligotrophic waters.

As seen in the oligotrophic hydrocasts, the POC maxima occur higher in the water column than the chlorophyll maxima and the peaks in Chl-a:C ratio correspond to the chlorophyll maxima. This further indicates that phytoplankton at the chlorophyll maximum are photoacclimated to low-light environments and are not the main source of primary production in the ocean.

Hydrocasts 020 and 023 had carbon and chlorophyll data that indicates they lie somewhere between the oligotrophic and eutrophic hydrocasts. However, the relationship between the POC, chlorophyll and Chl-a:C profiles follow the same pattern seen in the eutrophic and oligotrophic hydrocasts.

Nitrogen ratios for all of the hydrocasts were very close to the Redfield ratio of 106 C: 16 N (6.625). This indicates that majority of the particulate organic carbon measured was part of living organisms at the time of sampling. The main deviation occurs in the deepest bottles of some of the hydrocasts. In several of the hydrocasts the C:N ratio increases significantly in bottles triggered below 200 m. These increases in C:N ratios correspond to spikes in POC in the same bottles. This shows a depletion of

nitrogen relative to carbon. In nitrogen-limited waters, this could indicate a scavenging of nitrogen by other organisms, showing that the organic carbon spike is due to an accumulation of senescent phytoplankton that are decomposing. Alternatively, the deep POC spike could be due to the deep scattering layer.

Consistent Chl-a:C ratios within each hydrocast were found only in the mixed layer depths. Overall, the Chl-a:C ratios vary significantly with depth and maximum Chl-a:C ratios vary significantly between hydrocasts. Additionally, significant variation was present in the surface stations. This increases the difficulty of estimating standing stock of carbon from satellite imagery. A chlorophyll to carbon mass ratio of 1/75 (0.01) is considered typical. The values found in this study vary between 0.001 and 0.022 for hydrocasts and between 0.0003 and 0.009 for surface stations. This shows that a fixed chlorophyll to carbon ratio cannot be used to produce standing stocks of carbon.

Conclusion

Remote sensing imagery has the potential to be a powerful tool in analysis of global-scale ocean processes. Our study establishes the relationship between satellite-derived surface chlorophyll values and *in-situ* surface and depth chlorophyll values. Satellite measurements can estimate surface chlorophyll in both oligotrophic and eutrophic waters, though it is more accurate in oligotrophic water. These surface values have been shown to correlate closely to the depth of the chlorophyll maximum and total integrated water column chlorophyll. Therefore, satellite imagery can accurately estimate chlorophyll profiles for open-ocean waters.

Additionally, fluorometry data strongly correlates with our *in-situ* chlorophyll measurements. Calibration of a fluorometer to our observed chlorophyll to fluorometer relationship would allow the estimation of chlorophyll values without obtaining discrete water samples.

However, despite the potential accuracy of satellite prediction of *in-situ* chlorophyll values, it is unlikely that accurate estimations of standing stock of carbon can be obtained from satellite imagery. We observed large variations in the chlorophyll to carbon ratio both by depth and by latitude. Also, the chlorophyll maximum was not found to coincide with the depth at which highest production is occurring. These relationships make it difficult to establish a connection between satellite data and *in-situ* organic carbon concentrations.

References

Antoine, D., J. M. Andre, and A. Morel. 1996. Oceanic primary production .2. Estimation at global scale from satellite (coastal zone color scanner) chlorophyll. Global Biogeochemical Cycles **10**:57-69.

Arrigo, K. R., G. R. DiTullio, R. B. Dunbar, et al. 2000. Phytoplankton taxonomic variability in nutrient utilization and primary production in the Ross Sea. Journal of Geophysical Research **105**:8827-8845.

Babin, M., A. Morel, and B. Gentili. 1996. Remote sensing of sea surface sun-induced chlorophyll fluorescence: consequences of natural variations in the optical characteristics of phytoplankton and the quantum yield of chlorophyll a fluorescence. International Journal of Remote Sensing **17**:2417-2448.

Behrenfeld, M. J., E. Boss, D. A. Siegel, et al. 2005. Carbon-based ocean productivity and phytoplankton physiology from space. Global Biogeochemical Cycles **19**.

Behrenfeld, M. J., and P. G. Falkowski. 1997. Photosynthetic rates derived from satellite-based chlorophyll concentration. Limnology and Oceanography **42**:1-20.

Bouman, H. A., T. Platt, S. Sathyendranath, et al. 2003. Temperature as indicator of optical properties and community structure of marine phytoplankton : implications for remote sensing. Marine Ecology Progress series **258**:19-30.

Campbell, J., D. Antoine, R. Armstrong, et al. 2002. Comparison of algorithms for estimating ocean primary production from surface chlorophyll, temperature, and irradiance - art. no. 1035. Global Biogeochemical Cycles **16**:1035.

Esaias, W. E., M. R. Abbott, I. Barton, et al. 1998. An overview of MODIS capabilities for ocean science observations. IEEE Transactions on Geoscience and Remote Sensing **36**:1250-1265.

Iverson, R. L., W. E. Esaias, and K. Turpie. 2000. Ocean annual phytoplankton carbon and new production, and annual export production estimated with empirical equations and CZCS data. Global Change Biology **6**:57-72.

Siegel, D. A., T. K. Westberry, M. C. O'Brien, et al. 2001. Bio-optical modeling of primary production on regional scales: the Bermuda BioOptics project. Deep-Sea Research Part Ii-Topical Studies in Oceanography **48**:1865-1896.

Appendix A. Surface station sampling locations

Station #	Date	Time	Log	Latitude	Longitude
SS-001a	14-May-05	1703	486.0	15°11.6' N	156°13.6' W
SS-002	14-May-05	2010	510.9	14°48.5' N	156°14.7' W
SS-003	15-May-05	1230	540.7	14°18.4' N	156°16.3' W
SS-004a	15-May-05	0410	550.0	14°7.1' N	156°19.5' W
SS-005	15-May-05	0750	574.4	13°43.7' N	156°20.8' W
SS-006a	15-May-05	1604	616.8	13°0.0' N	156°24.9' W
SS-007	15-May-05	1953	646.0	12°32.5' N	156°22.5' W
SS-008	16-May-05	0021	673.0	12°5.1' N	156°23.5' W
SS-009a	16-May-05	0432	684.6	11°50.4' N	156°25.2' W
SS-010	16-May-05	0800	707.8	11°27.4' N	156°24.9' W
SS-011	16-May-05	1725	751.1	10°40.1' N	156°27.4' W
SS-012	16-May-05	2025	769.9	10°19.2' N	156°26.7' W
SS-013	16-May-05	2335	784.8	10°3.4' N	156°28.4' W
SS-014a	17-May-05	0400	806.7	9°39.8' N	156°28.5' W
SS-015	17-May-05	0800	834.4	9°10.6' N	156°29.1' W
SS-016a	17-May-05	1615	890.5	8°30.1' N	156°33.5' W
SS-017	17-May-05	2000	not streamed	8°6.2' N	156°34.7' W
SS-018	18-May-05	0008	896.1	7°55.3' N	156°38.6' W
SS-019a	18-May-05	0405	915.1	7°34.3' N	156°44.1' W
SS-020	18-May-05	0800	934.3	7°18.1' N	156°48.6' W
SS-021a	18-May-05	1645	966.8	6°44.2' N	156°55.5' W
SS-022	18-May-05	2000	993.6	6°17.6' N	157°0.3' W
SS-023	19-May-05	0022	999.0	6°11.0' N	157°1.5' W
SS-024a	19-May-05	0400	1013.8	5°42.2' N	157°1.6' W
SS-025	19-May-05	0814	1032.0	5°34.8' N	157°3.8' W

SS-026a	19-May-05	1728	1046.2	5°14.5' N	157°5.5' W
SS-027	19-May-05	2000	1063.4	4°37.1' N	157°0.4' W
SS-028	20-May-05	0000	1075.0	4°45.8' N	157°11.0' W
SS-029a	20-May-05	0405	1098.5	4°23.0' N	157°13.9' W
SS-030	20-May-05	0800	1127.5	3°54.0' N	157°16.9' W
SS-031a	20-May-05	1600	1150.8	3°24.9' N	157°20.3' W
SS-032	20-May-05	1935	1174.0	3°4.3' N	157°27.4' W
SS-033	21-May-05	0000	1214.6	2°30.1' N	157°38.2' W
SS-034a	21-May-05	0400	1239.3	2°7.2' N	157°36.1' W
SS-035	23-May-05	2020	1257.5	2°10.2' N	157°38.4' W
SS-036	24-May-05	0000	1291.0	2°32.5' N	158°1.3' W
SS-037a	24-May-05	0406	1329.7	2°57.0' N	158°28.1' W
SS-038a	24-May-05	0800	1355.0	3°12.2' N	158°45.9' W
SS-039a	24-May-05	0000	1361.7	3°22.3' N	158°54.3' W
SS-040	24-May-05	2000	1370.2	3°28.7' N	159°1.8' W
SS-041	24-May-05	2353	1379.0	3°32.9' N	159°6.0' W
SS-042a	25-May-05	0400	1389.5	3°42.1' N	159°14.4' W
SS-038b	24-May-05	0800	1355.0	3°12.2' N	158°45.9' W
SS-017 Blank					
SS-030 Blank		0800			
SS-039 Blank					
SS-017 Blank	17-May-05				
SS-011a	16-May-05				
SS-001b	14-May-05	1703	486.0	15°11.6' N	156°13.6' W
SS-004b	15-May-05	0410	550.0	14°7.1' N	156°19.5' W
SS-006b	15-May-05	1604	616.8	13°0.0' N	156°24.9' W
SS-009b	16-May-05	0432	684.6	11°50.4' N	156°25.2' W

SS-014b	17-May-05	0400	806.7	9°39.8' N	156°28.5' W
SS-016b	17-May-05	1615	890.5	8°30.1' N	156°33.5' W
SS-019b	18-May-05	0405	915.1	7°34.3' N	156°44.1' W
SS-021b	18-May-05	1645	966.8	6°44.2' N	156°55.5' W
SS-024b	19-May-05	0400	1013.8	5°42.2' N	157°1.6' W
SS-026b	19-May-05	1728	1046.2	5°14.5' N	157°5.5' W
SS-029b	20-May-05	0405	1098.5	4°23.0' N	157°13.9' W
SS-031b	20-May-05	1600	1150.8	3°24.9' N	157°20.3' W
SS-034b	21-May-05	0400	1239.3	2°7.2' N	157°36.1' W
SS-037b	24-May-05	0406	1329.7	2°57.0' N	158°28.1' W
SS-039b	24-May-05	0000	1361.7	3°22.3' N	158°54.3' W
SS-042b	25-May-05	0400	1389.5	3°42.1' N	159°14.4' W

Appendix B. Hydrocast sampling locations

Station #	Date	Time	Log	Latitude	Longitude
HC-010	14-May-05	1206	460.0	15°38.8' N	156°4.8' W
HC-013	15-May-05	1200	597.6	13°19.7' N	156°22.5' W
HC-016	16-May-05	1140	730.0	11°5.6' N	156°22.5' W
HC-020	17-May-05	1156	853.9	8°50.5' N	156°30.8' W
HC-023	18-May-05	1232	943.5	7°6.2' N	156°51.5' W
HC-026	19-May-05	1208	1040.1	5°23.5' N	157°4.0' W
HC-029	20-May-05	1200	1139.9	3°38.8' N	157°17.9' W
HC-032	24-May-05	1200	1358.0	3°15.2' N	158°47.7' W

.

Appendix C. Hydrocast data

Hydrocast#	Depth	Chl-a Rep A (ug/L)	Chl-a Rep B (ug/L)	Avg Chl-a (ug/L)	% diff b/w A and B	POC (ug/L)	PON (ug/L)	Satellite Chl value (ug/L)	C:N ratio
HC-010	0.0	1.9E-02	2.8E-02	0.0235	38.30			**0.0553**	
HC-010	24.7	2.9E-02	4.0E-02	0.0345	31.88	13.84	2.62	**0.0553**	6.16
HC-010	50.1	6.0E-02	3.2E-02	0.046	60.87	27.11	4.75	**0.0553**	6.66
HC-010	74.2	7.0E-02	7.2E-02	0.071	2.82	25.81	4.54	**0.0553**	6.64
HC-010	99.3	1.3E-01	8.1E-02	0.107	48.60	29.17	5.7	**0.0553**	5.97
HC-010	124.9	2.5E-01	2.3E-01	0.242	7.44	20.62	4.09	**0.0553**	5.88
HC-010	148.5	2.6E-01	1.3E-01	0.1955	65.98	21.05	3.41	**0.0553**	7.20
HC-010	192.0	4.1E-02	4.9E-02	0.045	17.78	25.28	4.18	**0.0553**	7.06
HC-013	0.0	2.4E-02	2.8E-02	0.026	15.38	11.87	2.95	**0.013**	4.69
HC-013	25.7	5.0E-03	2.6E-02	0.0155	135.48	15.54	2.68	**0.013**	6.77
HC-013	50.5	3.1E-02	3.7E-02	0.034	17.65	17.8	2.99	**0.013**	6.95
HC-013	74.8	8.4E-02	7.3E-02	0.0785	14.01	16.69	3	**0.013**	6.49
HC-013	108.8	7.3E-02	3.6E-02	0.0545	67.89	18.46	3.25	**0.013**	6.63
HC-013	143.7	1.6E-01	1.4E-01	0.151	14.57	11.61	1.96	**0.013**	6.90
HC-013	169.1	1.2E-01	1.2E-01	0.119	1.68	7.93	1.63	**0.013**	5.69
HC-013	285.0	2.0E-03	2.0E-03	0.002	0.00	22.26	2.48	**0.013**	10.45
HC-016	0.0	4.2E-02	2.9E-02	0.0355	36.62	13.18	2.69	**0.0471**	5.72
HC-016	25.6	4.2E-02	3.8E-02	0.04	10.00	16.82	3.02	**0.0471**	6.49
HC-016	50.6	4.4E-02	3.8E-02	0.041	14.63	18.1	2.85	**0.0471**	7.39
HC-016	74.5	9.0E-02	5.6E-02	0.073	46.58	16.8	3.16	**0.0471**	6.20
HC-016	99.2	1.5E-01	1.5E-01	0.1515	1.98	19.27	4.2	**0.0471**	5.36
HC-016	124.7	1.7E-01	3.0E-01	0.232	56.03	15.33	3.31	**0.0471**	5.40

HC-016	148.7	2.4E-01	2.3E-01	0.2345	1.28	10.79	2.45	**0.0471**	5.13
HC-016	244.0	3.0E-03	7.0E-03	0.005	80.00	14.52	4.38	**0.0471**	3.86
HC-020	0	1.0E-01	1.3E-01	0.1165	28.33	22.72	5.40	**0.1411**	4.90
HC-020	25.2	1.0E-01	1.2E-01	0.1095	17.35	31.12	6.69	**0.1411**	5.42
HC-020	49.7	7.8E-02	1.2E-01	0.0985	41.62	40.38	9.11	**0.1411**	5.17
HC-020	74.3	1.5E-01	1.4E-01	0.146	2.74	26.42	5.85	**0.1411**	5.27
HC-020	99.1	1.4E-01	2.2E-01	0.181	43.09	26.31	6.16	**0.1411**	4.98
HC-020	123.8	1.2E-01	1.5E-01	0.1345	27.51	14.61	3.48	**0.1411**	4.90
HC-020	149.0	7.7E-02	5.5E-02	0.066	33.33	12.52	3.26	**0.1411**	4.48
HC-020	248.0	1.1E-02	8.0E-03	0.0095	31.58	33.38	7.78	**0.1411**	5.01
HC-023	0.0	2.4E-01	2.4E-01	0.239	3.35	27.46	6.01	**0.2648**	5.33
HC-023	24.8	3.6E-01	3.6E-01	0.3605	0.83	49.18	8.81	**0.2648**	6.51
HC-023	49.6	3.0E-01	3.5E-01	0.3235	17.62	42.38	8.22	**0.2648**	6.01
HC-023	74.9	3.4E-01	3.0E-01	0.317	12.62	28.82	6.20	**0.2648**	5.42
HC-023	99.5	1.4E-01	9.9E-02	0.118	32.20	15.06	3.23	**0.2648**	5.44
HC-023	124.8	3.9E-02	2.3E-02	0.031	51.61	8.90	2.35	**0.2648**	4.41
HC-023	148.3	2.5E-02	4.4E-02	0.0345	55.07	9.20	2.15	**0.2648**	5.00
HC-023	259.7	6.0E-03	6.0E-03	0.006	0.00	33.71	14.45	**0.2648**	2.72
HC-026		1.9E-01	2.4E-01	0.215	25.12	22.94	5.79	**0.23**	4.62
HC-026	21.1	1.9E-01	3.3E-01	0.2595	55.11	41.59	8.99	**0.23**	5.40
HC-026	39.8	3.6E-01	3.3E-01	0.3465	8.95	32.25	0.85	**0.23**	5.49
HC-026	59.7	3.6E-01	4.1E-01	0.38	13.16	23.82	5.84	**0.23**	4.76
HC-026	89.3	2.9E-01	2.8E-01	0.2865	3.14	14.19	3.13	**0.23**	5.28
HC-026	119.3	8.6E-02	9.5E-02	0.0905	9.94	10.22	2.74	**0.23**	4.36
HC-026	149.3	2.9E-02	2.3E-02	0.026	23.08	10.35	2.55	**0.23**	4.73
HC-026	302.0	6.0E-03	4.0E-03	0.005	40.00	25.01	3.11	**0.23**	9.37
HC-029	0.0	1.6E-01	1.7E-01	0.1655	1.81	28.09	5.96	**0.1745**	5.50

HC-029	20.2	1.6E-01	1.9E-01	0.177	14.69	33.16	6.32	**0.1745**	6.12
HC-029	40.2	2.0E-01	1.9E-01	0.1925	2.60	34.38	6.87	**0.1745**	5.84
HC-029	59.8	2.4E-01	2.3E-01	0.236	2.54	30.62	6.26	**0.1745**	5.70
HC-029	90.3	3.2E-01	2.3E-01	0.2735	31.81	21.59	4.72	**0.1745**	5.34
HC-029	120.2	6.8E-02	6.3E-02	0.0655	7.63	11.21	2.39	**0.1745**	5.48
HC-029	150.1	8.0E-03	9.0E-03	0.0085	11.76	8.12	1.32	**0.1745**	7.19
HC-029	222.9	3.0E-03	4.0E-03	0.0035	28.57	20.44	3.04	**0.1745**	7.84
HC-032	0.0	1.6E-01	1.8E-01	0.169	7.10	33.36	6.61	**NA**	5.88
HC-032	20.3	1.6E-01	1.9E-01	0.177	16.95	41.25	7.88	**NA**	6.11
HC-032	39.8	2.6E-01	3.1E-01	0.287	16.72	40.60	7.95	**NA**	5.95
HC-032	60.2	3.4E-01	3.5E-01	0.3455	2.03	33.11	6.42	**NA**	6.01
HC-032	89.4	2.5E-01	2.8E-01	0.264	11.36	30.31	6.12	**NA**	5.78
HC-032	119.7	9.4E-02	1.2E-01	0.1055	21.80	13.40	2.38	**NA**	6.56
HC-032	149.1	2.1E-02	2.4E-02	0.0225	13.33	12.30	2.07	**NA**	6.93
HC-032	260.0	6.0E-03	4.0E-03	0.005	40.00			**NA**	

Appendix D. Surface Station data.

Station #	Chl-a Rep A (ug/L)	Chl-a Rep B (ug/L)	Avg chl-a (ug/L)	% diff b/w A and B	POC (ug/L)	Avg POC (ug/L)	% diff b/w rep POC	PON (ug/L)	Avg PON (ug/L)	C:N ratio	Satellite Value
SS-001a	0.026	0.042	0.034	47.06	15.88	19.37	35.99	2.79	3.15	6.65	**0.0519**
SS-001b					22.85			3.51		7.60	**0.0519**
SS-002	0.024	0.020	0.022	18.18	19.66	19.66		3.29	3.29	6.97	**0.0522**
SS-003	0.013	0.022	0.0175	51.43	18.72	18.72		2.95	2.95	7.40	**0.0689**
SS-004a	0.020	0.014	0.017	35.29	13.27	15.30	26.48	1.97	2.90	7.87	**0.0284**
SS-004b					17.32			3.82		5.29	**0.0284**
SS-005	0.025	0.016	0.0205	43.90	17.49	17.49		2.68	2.68	7.60	**0.05**
SS-006a	0.006	0.011	0.0085	58.82	15.90	15.24	8.73	3.29	3.30	5.64	**0.026**
SS-006b					14.57			3.30		5.14	**0.026**
SS-007	0.015	0.019	0.017	23.53	16.48	16.48		2.88	2.88	6.67	**0.019**
SS-008	0.019	0.016	0.0175	17.14	14.86	14.86		3.20	3.20	5.41	**0.0141**
SS-009a	0.014	0.030	0.022	72.73	14.29	13.68	8.92	2.56	2.60	6.50	**0.0416**
SS-009b					13.07			2.63		5.80	**0.0416**
SS-010	0.032	0.023	0.0275	32.73	18.85	18.85		2.97	2.97	7.39	**0.0351**
SS-011	0.026	0.023	0.0245	12.24	14.69	14.45		2.56	2.74	6.70	**0.0612**
SS-012	0.042	0.007	0.0245	142.86	14.37	14.37		2.41	2.41	6.95	**0.0297**
SS-013	0.021	0.025	0.023	17.39	20.39	20.39		3.59	3.59	6.62	**0.0284**
SS-014a	0.100	0.066	0.083	40.96	23.42	24.60	9.59	4.53	5.08	6.03	**0.0427**
SS-014b					25.78			5.62		5.35	**0.0427**
SS-015	0.145	0.114	0.1295	23.94	26.83	26.83		5.40	5.40	5.80	**0.1071**
SS-016a	0.148	0.105	0.1265	33.99	28.92	31.84	18.34	5.05	5.52	6.67	**0.155**
SS-016b					34.76			5.98		6.78	**0.155**

SS-017	0.161	0.253	0.207	44.44	25.46	25.46		5.24	5.24	5.67	**0.129**
SS-018	0.159	0.130	0.1445	20.07	25.43	25.43		5.31	5.31	5.58	**0.1175**
SS-019a	0.127	0.166	0.1465	26.62	44.93	42.41	11.88	8.36	8.10	6.27	**0.235**
SS-019b					39.89			7.84		5.93	**0.235**
SS-020	0.173	0.181	0.177	4.52	40.70	40.70		8.68	8.68	5.47	**0.2491**
SS-021a	0.231	0.210	0.2205	9.52	42.14	41.98	0.79	9.31	9.32	5.28	**0.2663**
SS-021b					41.81			9.33		5.23	**0.2663**
SS-022	0.218	0.218	0.218	0.00	38.27	38.27		7.86	7.86	5.68	**0.2093**
SS-023	0.189	0.127	0.158	39.24	36.76	36.76		7.66	7.66	5.60	**0.3038**
SS-024a	0.097	0.142	0.1195	37.66	37.88	38.89	5.17	7.97	8.01	5.54	**0.2773**
SS-024b					39.89			8.04		5.78	**0.2773**
SS-025	0.033	0.087	0.06	90.00	21.55	21.55		4.77	4.77	5.27	**0.2466**
SS-026a	0.109	0.102	0.1055	6.64	31.82	33.58	10.48	6.03	6.38	6.15	**0.258**
SS-026b					35.34			6.73		6.13	**0.258**
SS-027	0.158	0.120	0.139	27.34	38.99	38.99		6.82	6.82	6.67	**0.2051**
SS-028	0.079	0.079	0.079	0.00	43.57	43.57		9.00	9.00	5.64	**0.1842**
SS-029a	0.154	0.094	0.124	48.39	28.21	28.21		6.04	6.04	5.45	**0.1832**
SS-029b											**0.1832**
SS-030	0.236	0.180	0.208	26.92	27.13	27.13		6.26	6.26	5.06	**0.1791**
SS-031a	0.093	0.097	0.095	4.21	17.66	24.41	55.28	3.14	4.85	6.56	**0.1943**
SS-031b					31.15			6.56		5.54	**0.1943**
SS-032	0.152	0.101	0.1265	40.32	35.03	35.03		6.86	6.86	5.95	**0.1766**
SS-033	0.141	0.133	0.137	5.84	26.49	26.49		5.47	5.47	5.64	**0.1878**
SS-034a	0.125	0.090	0.1075	32.56	28.12	27.24	6.50	6.41	5.75	5.12	**0.2216**
SS-034b					26.35			5.08		6.05	**0.2216**
SS-035	0.086	0.071	0.0785	19.11	30.52	30.52	16.22	5.82	5.82	6.12	**0.2282**
SS-036	0.113	0.069	0.091	48.35	35.47			7.42		5.57	**NA**

SS-037a	0.146	0.068	0.107	72.90	22.83	26.02	24.49	5.51	5.92	4.83	**NA**
SS-037b					29.20			6.32		5.39	**NA**
SS-038a	0.119	0.171	0.145	35.86	22.66	27.51		5.02	5.83	5.26	**NA**
SS-039a	0.080	0.100	0.09	22.22	47.87	54.60	24.65	9.79	10.41	5.70	**NA**
SS-039b					61.33			11.02		6.49	**NA**
SS-040	0.150	0.054	0.102	94.12	37.55	37.55		7.45	7.45	5.88	**NA**
SS-041	0.124	0.101	0.1125	20.44	39.62	39.62		8.08	8.08	5.72	**NA**
SS-042a	0.096	0.056	0.076	52.63	30.77	29.33	9.82	6.08	6.10	5.90	**NA**
SS-042b					27.89			6.11		5.32	**NA**
SS-038b			0		32.36			6.63		5.70	**NA**
SS-017 Blank					3.81	3.43	40.55	0.84	1.01	5.27	**NA**
SS-030 Blank					2.42			1.14		2.47	**NA**
SS-039 Blank					3.99			1.22		3.83	**NA**
SS-017 Blank					3.49			0.85		4.81	**NA**
SS-011a					14.21			2.91		5.69	**NA**

Appendix E. Integrated Chl-a profiles for Hydrocast stations

Hydrocast#	Latitude	Bottle 13 (surface) Chl-a value	Int Chl (ug/10cm^2)	Surface Sat Chl-a (ug/L)	Integrated Chl from Calibrated Fluorescence (ug/10cm^2)
HC-010	15.64667	0.0235	20.24298	0.0553	28.89516447
HC-013	13.32833	0.026	18.80188	0.013	28.17715536
HC-016	11.09333	0.0355	28.01358	0.0471	30.487019
HC-020	8.841667	0.1165	22.61773	0.1411	35.71402311
HC-023	7.103333	0.239	34.27855	0.2648	48.40397568
HC-026	5.391667	0.215	37.5343	0.23	39.98371129
HC-029	3.646667	0.1655	25.73498	0.1745	40.24727654
HC-030	3.253333	0.169	32.3905	**unavailable**	39.225136
Correlation Coeff. with Bottle 13			0.822		0.964264305
Correlation Coeff. with Satellite		0.98	0.808		0.964437843